Chemosphere 287 (2022) 132020

Contents lists available at ScienceDirect

Chemosphere

journal homepage: www.elsevier.com/locate/chemosphere

Acid leaching of $LiCoO_2$ enhanced by reducing agent. Model formulation and validation

M.M. Cerrillo-Gonzalez, M. Villen-Guzman *, C. Vereda-Alonso, J.M. Rodriguez-Maroto, J. M. Paz-Garcia

Department of Chemical Engineering, University of Malaga, Malaga, Spain

HIGHLIGHTS

- A model to describe the acidic-reductive leaching of $LiCoO_2$ is presented.
- H_2O_2 is selected as reducing agent to enhance the extraction yields.
- The model is based on the formation of a Co_3O_4 insoluble crust around the particle.
- The model predicts the switch of controlling mechanisms from kinetics to mass transfer.
- The model has been validated with a set of 12 experiments at different conditions.

ARTICLE INFO

Handling Editor: Y Yeomin Yoon

Keywords:
Lithium-ion batteries recycling
Reductive leaching
H_2O_2
Shrinking core

ABSTRACT

In this work, a model has been formulated to describe the complex process of $LiCoO_2$ leaching through the participation of competing reactions in acid media including the effect of H_2O_2 as reducing agent. The model presented here describes the extraction of Li and Co in the presence and absence of H_2O_2, and it takes into account the different phenomena affecting the controlling mechanisms. In this context, the model predicts the swift from kinetic control to diffusion control. The model has been implemented and solved to simulate the leaching process. To validate the model and to estimate the model parameters, a set of 12 (in triplicate) extraction experiments were carried out varying the concentration of hydrochloric acid (within the range of 0.5–2.5 M) and hydrogen peroxide (range 0–0.6%v/v). The simulation results match fairly well with the experimental data for a wide range of conditions. Furthermore, the model can be used to predict results with different solid-liquid ratios as well as different acid and oxygen peroxide concentrations. This model could be used to design or optimize a $LiCoO_2$ extraction process facilitating the corresponding economical balance of the treatment.

1. Introduction

Lithium-ion batteries (LIBs) play an important role in the ecological transition towards a global decarbonized energy scheme. Until recently, LIBs were only used in portable electronic devices, but their technical features have made them attractive for electric transport and stationary energy storage (Velázquez-Martínez et al., 2019). It is estimated that the global demand for batteries will increase 14 fold by 2030 (compared to 2018 market), and electric vehicles are projected to require the 90% of that amount (Tsiropoulos et al., 2018). Such exponential growth of LIBs' use comes together with an increase of the demand of raw materials as well as an increase of the environmental impact associated with the manufacture of the batteries and their waste management.

The European Commission identifies the list of Critical Raw Materials (CRMs) to promote circular economy and to reduce the dependency on strategic raw materials (European Commission, 2008). This classification is based on the current and future evaluation of both the supply risk and the economic importance. As new information on the environmental impact of materials and technological advances appears, it is necessary to revise the CRMs list. The most recent list (2020) includes some of the most common raw materials used in LIBs such as cobalt, phosphorous, magnesium, natural graphite, and lithium (Amato et al.,

* Corresponding author.
E-mail address: mvillen@uma.es (M. Villen-Guzman).

https://doi.org/10.1016/j.chemosphere.2021.132020
Received 6 July 2021; Received in revised form 21 August 2021; Accepted 23 August 2021
Available online 25 August 2021

2021). These materials are, therefore, bottlenecks for the Li-ion battery EU supply (Valero et al., 2018). It should be note that approximately 74% of all battery materials are supplied by China, Africa, and Latin America. With regard to the production, China ranks first in the world, providing around 66% of finished LIBs while the EU currently produces less than 1%. (European Commission, 2020). Hence, selective metal recovery from LIBs' residue should be promoted to reduce the criticality of these materials and to follow a circular economy perspective.

For a sustainable development of the LIB technologies, it is essential to develop effective and efficient recycling treatments. The current recycling treatments combine the use of both physical and chemical processes. Physical processes, such as dismantling, crushing, sieving and thermal-mechano-chemical treatments, are used as a pre-treatment to improve the efficiency (Lv et al., 2018). The chemical processes aim the extraction, separation, and purification of the different valuable components. Pyrometallurgical and hydrometallurgical methods are the most commonly used. The latter are based on the recovery of metals via acidic leaching and selective precipitation [8]. Hydrometallurgical processes present relevant advantages, such as low energy consumption, high metal recovery rate (including Li) and high product purity. Hydrometallurgical methods can be combined and enhanced with green approaches, such as the use of deep eutectic solvents for the leaching or electrodialysis treatment for the selective separation, to further develop the technique and to be more environmentally friendly (Lv et al., 2018; Roy et al., 2021; Zheng et al., 2018).

As mentioned before, the first step in the hydrometallurgical process is leaching, which involves the dissolution of the solid particles or the extraction of the metals from them using a suitable solvent. The leaching step requires the addition of reactants such as strong acids and reducing agents to dissolve the solid particles and extract the valuable metals (Esmaeili et al., 2020). Obviously, the recycling process will only be feasible if the environmental impact and the cost related to the required reactants is low.

To optimize the hydrometallurgical process, the different reactions and mechanisms taking place during the leaching step should be deeply understood. Different models have been proposed to describe the dissolution-extraction reactions through solid-liquid interactions. Among them, two of the most widely used are the shrinking core model (SCM) and the shrinking particle model (SPM) (Chabhadiya et al., 2021; Ghassa et al., 2020; Jiang et al., 2018; Levenspiel, 1999; Porvali et al., 2020; Villen-Guzman et al., 2020; Zhang et al., 2015). Although these models have been widely applied to study liquid–solid systems as leaching kinetics in hydrometallurgical processes it should be noted that some assumptions within their formulation could not be valid in the dissolution-extraction of $LiCoO_2$ particles. For example, SCM models were developed to describe gas–solid systems assuming there must be a sharp interface between the reactant and the product layer. This condition has been overlooked in SCM models applied to leaching processes since microscopic examination should be required to determine whether there is a diffuse reaction zone or a definite product-reactant interface (Liddell, 2005). Furthermore, although numerous studies are focused on the determination of the rate-limiting step (diffusion film, chemical reaction control step or residue layer diffusion control step) and their respective activation energy, there is a lack of studies that deals with the evaluation of the leaching kinetics of metals (Gao et al., 2018). Therefore, the description of models based on the leaching reaction, considering the different parameters involved in the leaching (such as acid concentration, S/L ratio and reductant concentration) could provide a better understanding of the reaction mechanisms during the process.

The evaluation of solid-liquid reaction kinetics has been carried out through modified-models based on the SCM and SPM. Setiawan et al. (2019) modified the SCM to include an equilibrium reaction to describe the kinetics of lithium and cobalt recovery from spent LIBs using acetic acid. Raschman et al. (2019) developed an extended SPM which takes into account the influence of the S/L ratio, the non-ideal behaviour of concentrates aqueous solution and the chemical reaction order. Gao et al. (2018) studied the role of the reducing agent in the leaching kinetics of LIBs cathode scrap using acetic acid. In their work, the kinetic analysis was carried out using the standard SCM to determine the rate-controlling step in the absence and presence of H_2O_2 during the leaching process. Their results indicated that the use of reducing agent can alter the rate-controlling step from residue layer diffusion to chemical control.

Table 1
Experiments and concentration of aqueous solutions.

H_2O_2 ↓	HCl →		
	0.5 M	1.5 M	2.5 M
0% (v/v) (0 mM)	E1	E2	E3
0.2% (v/v) (86 mM)	E4	E5	E6
0.4% (v/v) (173 mM)	E7	E8	E9
0.6% (v/v) (260 mM)	E10	E11	E12

In a previous work (Cerrillo-Gonzalez et al., 2020a), the authors developed a mathematical model to describe the mechanisms of $LiCoO_2$ leaching in acid media, studying the controlling mechanisms (kinetics or diffusion) as a function of the thickness of the outer Co_3O_4 crust, based on the following two reactions deduced from experimental observations:

$$LiCoO_2(s) + 2H^+ \rightarrow Li^+ + \frac{1}{2}Co^{2+} + \frac{1}{6}Co_3O_4(s) + H_2O + \frac{1}{6}O_2 \quad (1)$$

$$Co_3O_4 + 6H^+ \rightarrow 3Co^{2+} + 3H_2O + \frac{1}{2}O_2 \quad (2)$$

The extraction of Li and Co from $LiCoO_2$ particles in an acid media involves the reduction of Co^{3+} to soluble Co^{2+}. In the absence of a stronger reducing agent, water oxidation half-reaction completes the redox pair. In this case, Li and Co are extracted from the particle leaving a residue of $Co_3O_4(s)$ (Cerrillo-Gonzalez et al., 2020b). From experimental results, it can be concluded that the acid dissolution of the $Co_3O_4(s)$ is significantly slower than the dissolution of $LiCoO_2(s)$. As a consequence, the $Co_3O_4(s)$ remains as a crust around the unreacted core of $LiCoO_2(s)$. This crust can limit the diffusion of the reactants from the aqueous solution to the surface of the unreacted core and apparently stop the reaction.

The presence of a strong reducing agent enhances the leaching process facilitating the reduction of Co^{3+} to soluble Co^{2+}. Despite hydrogen peroxide is widely known as an oxidizing agent, its use as a reducing agent here is justified due to the high reduction potential of Co^{3+}, and the fact that it does not introduce additional ions to the system. Accordingly, in this work, the previous model has been extended to assume that, in the presence of H_2O_2, the following reactions take place, simultaneously with the reactions (1) and (2):

$$LiCoO_2 + 3H^+ + \frac{1}{2}H_2O_2 \rightleftarrows Li^+ + Co^{2+} + 2H_2O + \frac{1}{2}O_2 \quad (3)$$

$$Co_3O_4 + 6H^+ + H_2O_2 \rightleftarrows 3Co^{2+} + 4H_2O + O_2 \quad (4)$$

In this work, the effect of the presence and absence of H_2O_2 on the leaching reaction kinetics of $LiCoO_2$ particle has been studied through the implementation of a physicochemical model. With the aim of validating the model, a set of extraction experiments were carried out varying the concentration of hydrochloric acid (within the range of 0.5–2.5 M) and hydrogen peroxide (range 0–0.6%v/v).

2. Materials and methods

2.1. Extraction experiments

Extraction experiments were carried out to evaluate the influence of the extracting and reducing agent concentration in the dissolution kinetics of $LiCoO_2$ (97% Alfa Aesar). The HCl and H_2O_2 were selected to

Table 2
Parameters used in simulation results.

Parameter	Value	Units	Description
k_1	2.17×10^{-8}	$(m\ s^{-1})$	Kinetic constant, equation (1)
k_2	8.33×10^{-9}	$\left(m^2 mol^{-2/3} s^{-1}\right)$	Kinetic constant, equation (2)
k_3	6.67×10^{-11}	$\left(m^5 mol^{-4/3} s^{-1}\right)$	Kinetic constant, equation (3)
k_4	1.67×10^{-12}	$\left(m^8 mol^{-8/3} s^{-1}\right)$	Kinetic constant, equation (4)
k_D	-3.2×10^7	(m^{-1})	Diffusion factor, equation (17)

act as extractant and reducing agent respectively, and the aqueous solutions used in each experiment are detailed in Table 1. The chosen values allow the study of excess, defect and approximately stoichiometric concentrations of HCl and H_2O_2 with respect to the initial amount of solid. Each experiment was carried out in triplicate.

The leaching process was performed in 100 mL Erlenmeyer flasks, where 2.5 g of solid and 50 mL of solution were added (*i.e.*, a S/L of 50 g/L). This experimental setup allows the free release of the oxygen produced in the reaction, avoiding overpressure inside the reactor. The suspensions were shaken with a magnetic stirring at 25 °C and atmospheric pressure which allows for perfect mixing hydraulic model.

Samples of 20 μL were collected at different times and diluted with 20 mL of 0.1 M HNO_3. The diluted samples were filtered using 0.6 μm glass-fiber and analysed via Atomic Absorption Spectrophotometry (Varian SpectrAA 1101) to quantify the amount of cobalt and lithium dissolved. The percentage of metal extracted was calculated according to:

$$x = \frac{C_{t,i} V_r}{m_{0,i}} \tag{5}$$

where x (wt%) is the percentage of metal extracted, $C_{t,\,i}$ $\left(mg\ L^{-1}\right)$ is the dissolved metal concentration, V_r (L) is the solution volume and $m_{0,\,i}$(mg) is the initial amount of metal in the solid sample. The total content of metal in the samples was in accordance with the stoichiometry of $LiCoO_2$, validated through microwave acid-assisted digestion (EPA method 3051A).

As pH meters were unsuitable due to the very low pH values, the concentration of hydroniums in the initial and final solution were determined by acid-base titration (Phenolphthalein, NaOH 1 M).

2.2. Physicochemical model

The model presented here is based on the following assumptions:

1. The extraction-dissolution of $LiCoO_2$ particles in an aqueous solution containing HCl and H_2O_2, takes place following the equations (1)–(4).
2. $LiCoO_2$ particles used are assumed to be spherical with a radius of $R_p = 5$ μm and uniform particle distribution, which is consistent with typical synthesis methods for LCO batteries (Nakamura and Kajiyama, 1999a, 1999b). The unreacted core radius, r_c(m), decreases during the reaction while R_p and the number of particles (n_p) remain constant. This means that the Co_3O_4 crust is porous, and that the porosity increases as the crust gets dissolved. The thickness of the crust is used to determine the resistance to the diffusion of species from the reactive core surface to the bulk solution (explained later in assumption 7). Therefore, this assumption is consistent with the observation of switch from chemical kinetics to diffusion transport controlling mechanism. In the case that the crust can be considered completely dissolved, $R_p = r_c$.
3. The kinetic rates for the reactions are given by:

$$r_1 = -k_1 \left(\frac{n_p 4\pi r_c^2}{V_r}\right) C_{H^+}^{core} \tag{6}$$

$$r_2 = -k_2 \left(C_{Co_3O_4}\right) \left(C_{H^+}^{core}\right)^{2/3} \tag{7}$$

$$r_3 = -k_3 \left(\frac{n_p 4\pi r_c^2}{V_r}\right) \left(C_{H^+}^{core}\right)^{1/3} \left(C_{H_2O_2}\right)^2 \tag{8}$$

$$r_4 = -k_4 \left(C_{Co_3O_4}\right) \left(C_{H^+}^{core}\right)^{2/3} \left(C_{H_2O_2}\right)^2 \tag{9}$$

where k_j ($j = 1$ to 4) are the kinetic constants (units in Table 2), V_r (m^3) is the reaction volume, and C_i stands for molar concentration (mol m^{-3}). $C_{H^+}^{core}$ is the concentration of protons in the position r_c. The reaction orders presented in the equations correspond to fitting parameters, as explained in the Results Section.

4. The production rates of Li^+, Co^{2+}, H^+ and H_2O_2, are given by:

$$r_{Li^+} = r_1 + r_3 \tag{10}$$

$$r_{Co^{2+}} = \frac{1}{2} r_1 + 3r_2 + r_3 + 3r_4 \tag{11}$$

$$r_{H^+} = -2r_1 - 6r_2 - 3r_3 - 6r_4 \tag{12}$$

$$r_{H_2O_2} = -\frac{1}{2} r_3 - r_4 \tag{13}$$

5. Water self-ionization reaction is included in the model, and it is supposed to be in equilibrium:

$$H_2O \rightleftarrows H^+ + OH^- \quad ; \quad K_w = 10^{-8}\ \text{(for concentrations in mM)} \tag{14}$$

6. The Davies equation for the activity factors is used:

$$\log \gamma_i = -A z_i^2 \left(\frac{\sqrt{I}}{1+\sqrt{I}} - 0.3 \cdot I\right) \tag{15}$$

where γ_i (−) is the activity factor, z_i (−) is the ionic charge of the species i, I (M) is the ionic strength, and $A = 0.5085$ ($M^{-1/2}$). The Davies equation is known to predict the activity coefficient of moderately high concentration solutions, up to ionic strengths of 0.5 M. Therefore, any correction due to higher ionic strengths is assumed to be equivalent to that ionic strength limit. This means that the model includes uncertainties, especially for the case of 1.5 and 2.5 M of HCl, but it was assumed a better approximation than using no activity factor model. Accordingly, in the simulations presented here, the activity factor was $\gamma_i \approx 0.75$ for monovalent ions, such as Li^+ or H^+, and $\gamma_i \approx 0.3$ for divalent ions, such as Co^{2+}.

7. As the outer porous crust of $Co_3O_4(s)$ forms, the size of particle remains constant. Diffusion of the common reactant, H^+, through the layer of $Co_3O_4(s)$ from the bulk solution to the surface of the unreacted core is described as:

$$V_r \frac{dC_{H^+}}{dt} = -\frac{D_{H^+}^{eff} \left(C_{H^+}^{bulk} - C_{H^+}^{core}\right)}{\left(R_p - r_c\right)} n_p \left(4\pi R_p r_c\right) \tag{16}$$

where $C_{H^+}^{bulk}$ is the concentration of protons in the bulk liquid, and $D_{H^+}^{eff}$($m^2\ s^{-1}$) is the effective diffusion coefficient of the proton through the layer of Co_3O_4. The effective diffusion coefficient is considered to change as the crust increases and decrease as the crust dissolves, according to the following expression:

$$D_{H^+}^{eff} = D_{H^+}\ \varepsilon \exp\left(k_D \left(R_p - r_c\right)(1-\varepsilon)\right) \tag{17}$$

where $D_{H^+} = 9.311 \times 10^{-9}$ $\left(m^2 s^{-1}\right)$ is the diffusion coefficient at infinite dilution (Vanýsek, 2013), ε (−) is the porosity, and k_D (m^{-1}) is a parameter that measures the increase of the resistance to the mass transport as the crust increases, as a consequence of changes in

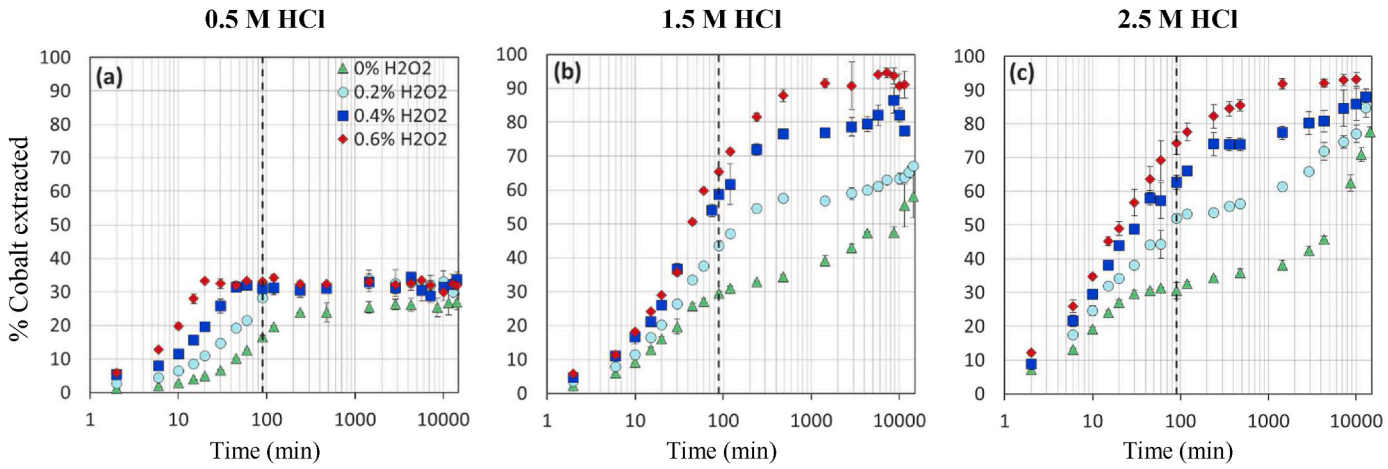

Fig. 1. Effect of H_2O_2 concentration on the extraction of cobalt at different HCl concentration: 0.5 M HCl (a), 1.5 M HCl (b) and 2.5 M HCl (c). (Conditions: solid/liquid ratio = 50 g/L; temperature = 25 °C).

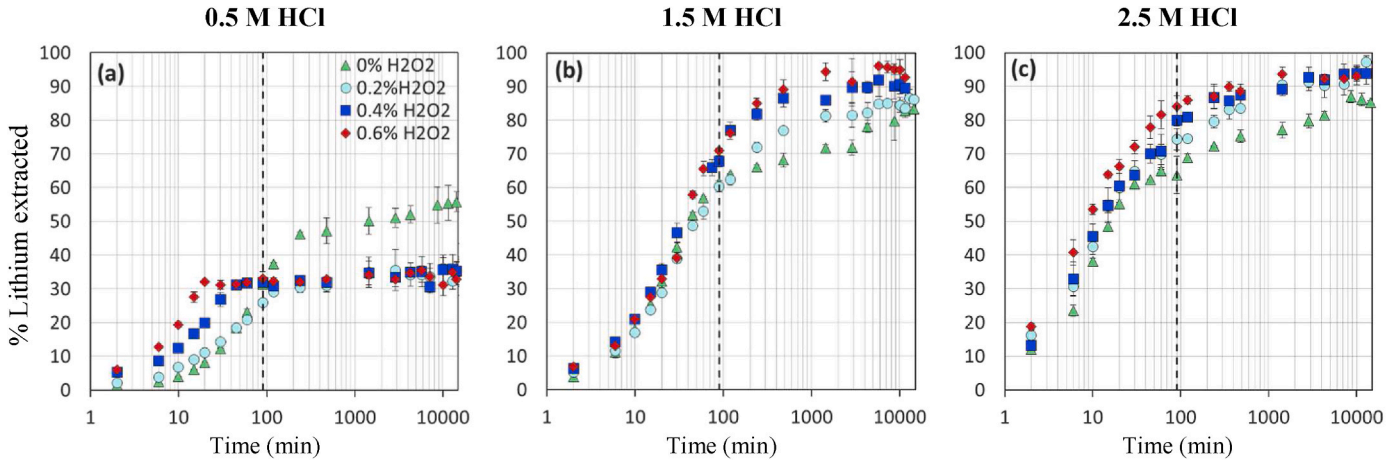

Fig. 2. Effect of H_2O_2 concentration on the extraction of lithium at different HCl concentration: 0.5 M HCl (a), 1.5 M HCl (b) and 2.5 M HCl (c). (Conditions: solid/liquid ratio = 50 g/L; temperature = 25 °C).

porosity or tortuosity, including pore closing due to counter diffusion of the O_2 gas formed in the reaction.

As the reaction proceeds and the outer $Co_3O_4(s)$ crust increases, the resistance to the diffusion transport increases according to eq. (17). At certain thickness of the crust, the process reaches a point in which the rate of proton diffusion is lower than the chemical kinetic consumption. At this point, as soon as protons reach the reactive surface they get consumed by the reaction.

8. The second Damköhler number, Da_{II} (−), defined in eq. (18) as the ratio of the chemical reaction rate to the mass transfer rate, is used to identify the controlling mechanisms.

$$Da_{II} = \frac{\text{kinetics rate}}{\text{diffussion rate}} \tag{18}$$

The diffusion rate is:

$$r_{1\,\text{diffusion}} = -\frac{D_{H^+}^{\text{eff}}\left(C_{H^+}^{bulk} - C_{H^+}^{core}\right)}{\left(R_p - r_c\right)} n_p (4\pi R r_c) \tag{19}$$

where, if $Da_{II} \leq 1$ then $C_{H^+}^{core} = C_{H^+}^{bulk}$, and the process rate is defined by the chemical kinetics law. However, whenever $Da_{II} > 1$ then $C_{H^+}^{core} = 0$, and the process rate is controlled by the diffusion. The reaction r_3, in equation (8), is treated similarly.

3. Results and discussion

For the discussion of the results, we will refer to "short time" to the first 90 min and "long time" to the final experiment time, 9 days. As this research is oriented to facilitate the industrial application of the technique, results in short times are more relevant and, therefore, the experiments will be discussed according to the extractions yields obtained at that point.

3.1. Experimental results

The experimental results are shown in Fig. 1 and Fig. 2 where the transient values of percentage for cobalt (Co) and lithium (Li) are presented, respectively.

Experimental results are in accordance with the model assumptions:

1. The extraction of Li and Co do not take place in a 1:1 proportion. Li is extracted in a higher amount than Co, and in a stoichiometric proportion near 2:1 in the absence of H_2O_2. It can be observed that, in the absence of H_2O_2, the total extraction of Li and Co in a short time is limited to approximately 50–60% and 25–30% respectively. This observation is consistent with the proposed equation (1).
2. The extraction shows a clear change of mechanism, not related to the depletion of reactants. It is observed that there is a change in the

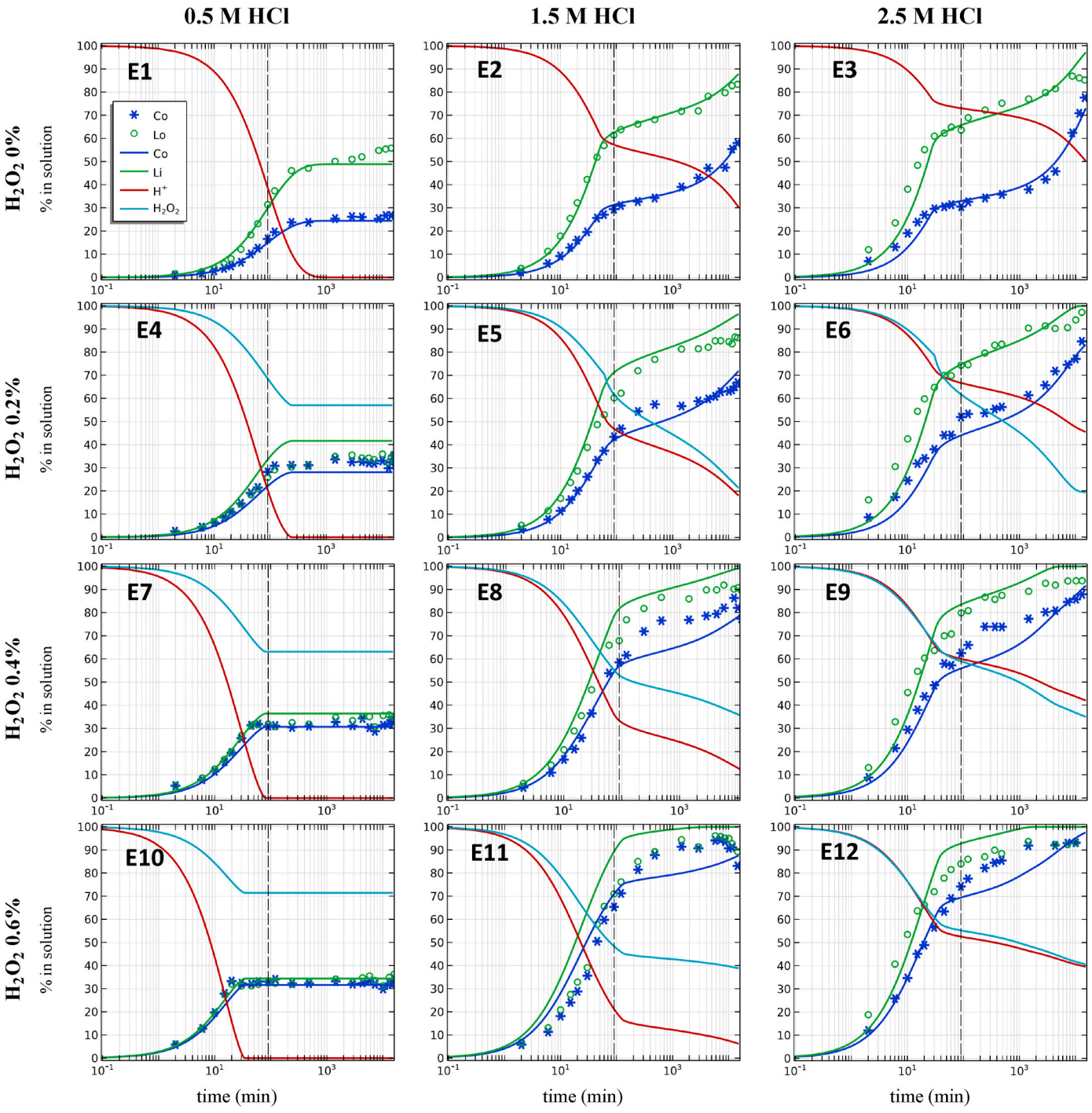

Fig. 3. Experimental (marks) and simulation (lines) results for E1-E2. In the case of Li and Co, the reference is the concentration in case of total extraction. In the case of HCl and H_2O_2, the reference is the initial concentration in the aqueous extracting solution.

tendency of the extraction rate, associated with the change of control mechanisms, from kinetic to diffusion control. As mentioned before, this is related to the formation of Co_3O_4 crust. Therefore, this observation is consistent with the formation of a diffusion limiting crust, as modelled in equation (2) and the equations 16–19.

3. Despite the extraction rate gets controlled by the diffusion of reactants through the outer crust, it is possible to achieve high extractions of both Li and Co in long time experiments. This indicates the effect of the reaction (2), that will promote the process to continue by slowly dissolving the outer crust of Co_3O_4. However, as mentioned before, for a reasonable up-scaling of the process to industrial scale, short time yields are more relevant.
4. The use of H_2O_2, increases both the proportion of extracted Li and Co to values near 1:1 and accelerates the extraction. This observation is consistent with the proposed equations (3) and (4).

In general, it can be observed that the extraction yields and rate increase with the concentration of acid and H_2O_2, except for the experiments using 0.5 M of HCl which were carried out using acid below the stoichiometric concentration.

Increasing H_2O_2 not only accelerates the extraction process, but it

also seems to reduce the effect of the formation of the Co_3O_4 outer crust, and therefore the effect of diffusive controlled kinetics is lower than experiments without the reducing agent. As expected, the higher extraction in the short time limit of 90 min occurs using HCl 2.5 M and 0.6%v/v H_2O_2, reaching to extraction of ≈ 85% of Li and ≈ 75% of Co.

3.2. Simulation results

Table 2 lists the parameters used in the simulations presented in this section. The Chemical Reaction Engineering module form the software COMSOL Multiphysics was used to obtain numerically integrate the kinetic equations and carry out the parameters' estimation study. The parameters listed in Table 2 resulted in the best fit of the model simulation and the experimental results.

Fig. 3 shows both experimental and simulation results for the 12 experiments carried out. The figure shows percentage of extracted Li and Co referred to the maximum extractable in the solid, and percentage of protons and hydrogen peroxide with respect to that initially in the solution in each case. The results for experiments E1 to E12 are shown separately, for a better appreciation of the fitting better experimental and simulation results in each case. Parameters in Table 2 were used to obtain the simulated results.

The simulation results presented in Fig. 3 match fairly well with the experimental data for the different combinations of HCl and H_2O_2 concentrations, using the same model parameters for all simulations. It can be observed that the fitting between the simulation and the experimental results is less precise at longer times and higher concentrations, which is consistent with the hypothesis of the model. On one hand, the formation of O_2 bubbles may affect the transport rates, and high concentrations may produce unprecise quantification of the activity factors. As short time results are considered more relevant for this research, the model parameters have been adjusted for a better fitting of the short time experimental results.

Comparing the experiments using 0.5 M HCl with H_2O_2, Li and Co are obtained in a proportion near 1:1, while the proportion was approximately 1:2 in the case without H_2O_2. Nevertheless, the use of H_2O_2 derived in lower total amount of Li extracted. All experiments in this case are not limited by the formation of the Co_3O_4 crust, but for the depletion of protons in the media, as can be seen in the simulation results for the protons profile. The lower extraction of Li using H_2O_2 is therefore explained by the fact that reaction (3) consumes more protons than reaction (1). In these cases, H_2O_2 seems to be in excess and it can be concluded that it is crucial to assure a proper proportion of both acid and H_2O_2 in order to achieve high extraction yields.

In the case of the experiments carried out using HCl 1.5 M and 2.5 M, the acid is in a concentration above the minimum stoichiometric, including the cases with H_2O_2. It can be observed that, in general, the higher the concentration of HCl and H_2O_2, the closer to a 1:1 proportion of Li and Co is obtained and the higher extraction is attained in shorter times.

It can also be observed that the addition of H_2O_2 promotes and accelerates the reaction rate, which agree with the results obtained by Gao et al. (2018). They evaluated the role of H_2O_2 in the leaching process and concluded that the introduction of a reducing agent accelerates the leaching rate but decreases the influence of the acid concentration. This observation is according to the results obtained in the parametric fitting: in the absence of H_2O_2 the partial order for HCl is 1 while in the presence of H_2O_2 is 1/3 (equation (6) and (8)).

4. Conclusions

The simulation results presented here match fairly well with the experimental data for a wide range of different combinations of HCl and H_2O_2 concentrations. This good fitting suggests that it is possible to use the model for predicting the experimental results for any combination of HCl and H_2O_2 concentrations within the range of 0–2.5 M of HCl and 0–0.6% of H_2O_2. Furthermore, the results indicate that the presented model could be used to predict results with different solid-liquid proportions as well as different acid and hydrogen peroxide concentrations. Accordingly, the model presented here could be used to design LIBs recycling processes optimizing the amount of reactants for the extractions. This aspect is particularly crucial to assure the economical balance of the recycling treatments.

Furthermore, the study presented here can be expanded to study the dissolution of different LIBs materials (such as NMC cathode material), using different extractant agents (such as nitric or sulfuric acid) and different reducing agents (such as cementation precipitation with, *e.g.*, solid Fe). The authors will address these options in future works.

Declaration of competing interest

The authors declare that they have no known competing financial interests or personal relationships that could have appeared to influence the work reported in this paper.

Acknowledgments

This work has received funding from the European Union's Horizon 2020 research and innovation programme under the Marie Skłodowska-Curie grant agreement No. 778045 and the "Proyectos I+D+i en el marco del Programa Operativo FEDER Andalucía 2014–2020", Project no. UMA18-FEDERJA-279. Cerrillo-Gonzalez acknowledges the FPU grant (FPU18/04295) obtained from the Spanish Ministry of Education. Funding for open access charge: Universidad de Málaga / CBUA.

References

Amato, A., Becci, A., Villen-Guzman, M., Vereda-Alonso, C., Beolchini, F., 2021. Challenges for sustainable lithium supply: a critical review. J. Clean. Prod. 300, 126954. https://doi.org/10.1016/j.jclepro.2021.126954.

Cerrillo-Gonzalez, M.M., Villen-Guzman, M., Acedo-Bueno, L.F., Rodriguez-Maroto, J.M., Paz-Garcia, J.M., 2020a. Hydrometallurgical extraction of Li and Co from LiCoO2 particles–experimental and modeling. Appl. Sci. 10, 6375. https://doi.org/10.3390/app10186375.

Cerrillo-Gonzalez, M.M., Villen-Guzman, M., Vereda-Alonso, C., Gomez-Lahoz, C., Rodriguez-Maroto, J.M., Paz-Garcia, J.M., 2020b. Recovery of Li and Co from LiCoO2 via hydrometallurgical–electrodialytic treatment. Appl. Sci. 10, 2367. https://doi.org/10.3390/app10072367.

Chabhadiya, K., Srivastava, R.R., Pathak, P., 2021. Two-step leaching process and kinetics for an eco-friendly recycling of critical metals from spent Li-ion batteries. J. Environ. Chem. Eng. 9, 105232. https://doi.org/10.1016/j.jece.2021.105232.

Esmaeili, M., Rastegar, S.O., Beigzadeh, R., Gu, T., 2020. Ultrasound-assisted leaching of spent lithium ion batteries by natural organic acids and H2O2. Chemosphere 254, 126670. https://doi.org/10.1016/j.chemosphere.2020.126670.

European Commission, 2020. Study on the EU's list of critical raw materials. https://doi.org/10.2873/11619.

European Commission, 2008. Directive 2008/98/EC of the European Parliament and of the Council of 19 November 2008 on Waste and the Repealing Certain Directives.

Gao, W., Song, J., Cao, H., Lin, X., Zhang, X., Zheng, X., Zhang, Y., Sun, Z., 2018. Selective recovery of valuable metals from spent lithium-ion batteries – process development and kinetics evaluation. J. Clean. Prod. 178, 833–845. https://doi.org/10.1016/j.jclepro.2018.01.040.

Ghassa, S., Farzanegan, A., Gharabaghi, M., Abdollahi, H., 2020. The reductive leaching of waste lithium ion batteries in presence of iron ions: process optimization and kinetics modelling. J. Clean. Prod. 262, 121312. https://doi.org/10.1016/j.jclepro.2020.121312.

Jiang, F., Chen, Y., Ju, S., Zhu, Q., Zhang, L., Peng, J., Wang, X., Miller, J.D., 2018. Ultrasound-assisted leaching of cobalt and lithium from spent lithium-ion batteries. Ultrason. Sonochem. 48, 88–95. https://doi.org/10.1016/J.ULTSONCH.2018.05.019.

Levenspiel, O., 1999. Chemical reaction engineering. Ind. Eng. Chem. Res. https://doi.org/10.1021/ie990488g.

Liddell, K.C., 2005. Shrinking core models in hydrometallurgy: what students are not being told about the pseudo-steady approximation. Hydrometallurgy 79, 62–68. https://doi.org/10.1016/j.hydromet.2003.07.011.

Lv, W., Wang, Z., Cao, H., Sun, Y., Zhang, Y., Sun, Z., 2018. A critical review and analysis on the recycling of spent lithium-ion batteries. ACS Sustain. Chem. Eng. 6, 1504–1521. https://doi.org/10.1021/acssuschemeng.7b03811.

Nakamura, T., Kajiyama, A., 1999a. Synthesis of LiCoO2 particles with uniform size distribution. J. Eur. Ceram. Soc. 19, 871–874. https://doi.org/10.1016/S0955-2219(98)00334-3.

Nakamura, T., Kajiyama, A., 1999b. Synthesis of LiCoO2 particles with uniform size distribution using hydrothermally precipitated Co3O4 fine particles. Solid State Ionics 123, 95–101. https://doi.org/10.1016/S0167-2738(99)00114-9.

Porvali, A., Chernyaev, A., Shukla, S., Lundström, M., 2020. Lithium ion battery active material dissolution kinetics in Fe(II)/Fe(III) catalyzed Cu-H2SO4 leaching system. Separ. Purif. Technol. 236, 116305. https://doi.org/10.1016/j.seppur.2019.116305.

Raschman, P., Popovič, Ľ., Fedoročková, A., Kyslytsyna, M., Sučik, G., 2019. Non-porous shrinking particle model of leaching at low liquid-to-solid ratio. Hydrometallurgy 190, 105151. https://doi.org/10.1016/j.hydromet.2019.105151.

Roy, J.J., Cao, B., Madhavi, S., 2021. A review on the recycling of spent lithium-ion batteries (LIBs) by the bioleaching approach. Chemosphere 282, 130944. https://doi.org/10.1016/j.chemosphere.2021.130944.

Setiawan, H., Petrus, H.T.B.M., Perdana, I., 2019. Reaction kinetics modeling for lithium and cobalt recovery from spent lithium-ion batteries using acetic acid. Int. J. Miner. Metall. Mater. 26, 98–107. https://doi.org/10.1007/s12613-019-1713-0.

Tsiropoulos, I., Tarvydas, D., Lebedeva, N., 2018. Li-ion batteries for mobility and stationary storage applications Scenarios for costs and market growth. https://doi.org/10.2760/87175.

Valero, Alicia, Valero, Antonio, Calvo, G., Ortego, A., 2018. Material bottlenecks in the future development of green technologies. Renew. Sustain. Energy Rev. 93, 178–200. https://doi.org/10.1016/j.rser.2018.05.041.

Vanýsek, P., 2013. Equivalent conductivity of electrolytes in aqueous solution. In: CRC Handbook of Chemistry and Physics. CRC Press, p. 76.

Velázquez-Martínez, O., Valio, J., Santasalo-Aarnio, A., Reuter, M., Serna-Guerrero, R., 2019. A critical review of lithium-ion battery recycling processes from a circular economy perspective. Batteries 5, 68. https://doi.org/10.3390/batteries5040068.

Villen-Guzman, M., Paz-Garcia, J.M., Arhoun, B., Cerrillo-Gonzalez, M.M., Rodriguez-Maroto, J.M., Vereda-Alonso, C., Gomez-Lahoz, C., 2020. Chemical reduction of nitrate by zero-valent iron: shrinking-core versus surface kinetics models. Int. J. Environ. Res. Publ. Health 17, 1241. https://doi.org/10.3390/ijerph17041241.

Zhang, X., Cao, H., Xie, Y., Ning, P., An, H., You, H., Nawaz, F., 2015. A closed-loop process for recycling LiNi1/3Co1/3Mn1/3O2 from the cathode scraps of lithium-ion batteries: process optimization and kinetics analysis. Separ. Purif. Technol. 150, 186–195. https://doi.org/10.1016/j.seppur.2015.07.003.

Zheng, X., Zhu, Z., Lin, X., Zhang, Y., He, Y., Cao, H., Sun, Z., 2018. A mini-review on metal recycling from spent lithium ion batteries. Engineering 4, 361–370. https://doi.org/10.1016/j.eng.2018.05.018.